Cell Biochem Biophys (2012) 64:29–44
DOI 10.1007/s12013-012-9364-z

ORIGINAL PAPER

Amyloid-Like Fibril Formation by Tachykinin Neuropeptides and Its Relevance to Amyloid β-Protein Aggregation and Toxicity

Pradeep K. Singh · Samir K. Maji

Published online: 25 May 2012

Abstract Protein aggregation and amyloid formation are associated with both pathological conditions in humans such as Alzheimer's disease and native functions such as peptide hormone storage in the pituitary secretory granules in mammals. Here, we studied amyloid fibrils formation by three neuropeptides namely physalaemin, kassinin and substance P of tachykinin family using biophysical techniques including circular dichroism, thioflavin T, congo red binding and microscopy. All these neuropeptides under study have significant sequence similarity with Aβ(25–35) that is known to form neurotoxic amyloids. We found that all these peptides formed amyloid-like fibrils in vitro in the presence of heparin, and these amyloids were found to be nontoxic in neuronal cells. However, the extent of amyloid formation, structural transition, and morphology were different depending on the primary sequences of peptide. When Aβ(25–35) and Aβ40 were incubated with each of these neuropeptides in 1:1 ratio, a drastic increase in amyloid growths were observed compared to that of individual peptides suggesting that co-aggregation of Aβ and these neuropeptides. The electron micrographs of these co-aggregates were dissimilar when compared with individual peptide fibrils further supporting the possible incorporation of these neuropeptides in Aβ amyloid fibrils. Further, the fibrils of these neuropeptides can seed the fibrils formation of Aβ40 and reduced the toxicity of preformed Aβ fibrils. The present study of amyloid formation by tachykinin neuropeptides is not only providing an understanding of the mechanism of amyloid fibril formation in general, but also offering plausible explanation that why these neuropeptide might reduce the cytotoxicity associated with Alzheimer's disease related amyloids.

Keywords Neuropeptides · Amyloids · Functions · Fibrils · Peptide

Abbreviations

CR	Congo red
ThT	Thioflavin T
GAGs	Glycosaminoglycans
CD	Circular dichroism
EM	Electron microscopy
AFM	Atomic force microscopy
TFE	Trifluoroethanol
DMEM	Dulbecco's modified Eagle's medium

Introduction

Several human diseases are associated with protein aggregation and amyloid fibril formation [1] including Alzheimer's, Parkinson's, and Type II diabetes. Amyloid fibrils possess many common physical properties including their cross-β-sheet structure [2, 3], binding to amyloid-specific dyes such as congo red (CR) [4] and thioflavin T (ThT) [5] and morphology consisting mostly of 2–3 protofilaments [6, 7]. Several proteins that are not apparently associated with amyloid diseases also can form amyloid-like fibrils in vitro lead to the hypothesis that amyloid formation is the generic property of polypeptide chains [1, 8]. Amyloids can also perform beneficial functions for the

Electronic supplementary material The online version of this article (doi:10.1007/s12013-012-9364-z) contains supplementary material, which is available to authorized users.

P. K. Singh · S. K. Maji (✉)
Department of Biosciences and Bioengineering and Wadhwani Research Centre for Biosciences and Bioengineering, IIT Bombay, Powai, Mumbai 400076, India
e-mail: samirmaji@iitb.ac.in

host organisms [1, 9] and are known as "functional amyloids" [10–12]. Recently it was shown that the protein/peptide hormones are stored inside the secretory granules as amyloid-like structure [13]. The discovery of diverse range of functional amyloids suggests that amyloid fold is capable of performing normal physiological functions. The nontoxicty of several amyloids, with their high stability and mechanical stiffness raise the possibility that amyloids could be useful for designing novel nanostructure materials for biomedical applications [14–18]. Here, we studied the aggregation and amyloid formation of three neuropeptides; physalaemin, kassinin, and substance P (sub-P) that belong to tachykinin family. Tachykinin family of neuropeptides are of ten to twelve residues long that exist from amphibians to mammals [19, 20] and share the consensus sequence of Phe–Xxx–Gly–Leu–Met–NH2 at C-terminus, where the Xxx represents either an aromatic (Phe or Tyr) or an aliphatic (Val or Ile) amino acid residue [21, 22]. These neuropeptides perform diverse functions that include exciting neurons, evoking behavioral responses, potent vasodilators, secretagogues and are involved in contraction of the smooth muscles [23, 24]. Out of these three neuropeptides under study, sub-P is of mammalian origin, however, kassinin and physalaemin are of amphibian origin [21]. The immunoelctron microscopic study with the tissue from spinal ganglia of rats showed sub-P immunoreactivity that are localized in large-electron dense granules [25] suggested that tachykinin peptides are stored in the secretory granules [26].

Interestingly, these tachykinin neuropeptides possess significant sequence similarity with the central region of Aβ (Aβ(25–35)), which forms amyloid fibrils and retains neurotoxicity as of full-length Aβ peptide [27, 28]. It was reported that presence of tachykinin peptides reduce the toxicity of Aβ(25–35) amyloids [27, 29]. However, the mechanism of neuroprotection by these peptides against Aβ(25-35) is largely unknown. Inspired by these observations and recent suggestions that peptide/proteins in neuroendocrine can form functional amyloid [13], we studied the amyloid formation by three tachykinin family of neuropeptides in the presence and absence of heparin using circular dichroism (CD), ThT, CR binding, electron microscopy (EM), and atomic force microscopy (AFM). All three neuropeptides formed amyloid-like fibrils in vitro. Kassinin and sub-P showed large structural transition and amyloid formation in vitro whereas physalaemin showed lesser tendency towards conformational transition and amyloid formation. Consistent with our in vitro data, amyloid prediction algorithm WALTZ also showed amyloid forming tendency of kassinin and sub-P. The fibrils of these peptides were nontoxic in SH-SY5Y cells and reduced the toxicity of preformed Aβ40 fibrils when mixed together. The co-aggregation studies of these neuropeptides with Aβ(25–35) and full-length Aβ40 have suggested accelerated formation of amyloids by 1:1 molar ratio of Aβ species and each of the neuropeptides than that of individual peptides. The co-aggregates showed different fibrillar morphology with reduced toxicity than the fibril formed by Aβ peptides. The fibrils of these neuropeptides also seed the fibril formation of Aβ40. The present study could offer not only the better understanding of the amyloid formation by peptides but also could suggest the possible role of tachykinin peptides in reducing Aβ toxicity.

Materials and Methods

Chemicals and Reagents

Chemicals/biochemicals were purchased from Sigma and were of the high purity. Water was double-distilled and deionized using a Milli-Q system (Millipore Corp., Bedford, MA). Peptides were purchased from BACHEM.

Peptide Fibril Formation

The peptides were dissolved in 0.5 mL of 5 % D-Mannitol, 0.01 % sodium azide, pH 5.5 at a concentration of 2 mg/mL in 1.5 mL eppendorf tubes. The eppendorf tubes containing peptide solutions were placed into an EchoTherm model RT11 rotating mixture (Torrey Pines Scientific, USA) with a speed corresponding 50 r.p.m. inside a 37 °C incubator. At suitable intervals, ThT, CD and EM were performed to analyze the aggregation. For aggregation studies in presence of heparin, all the peptides were dissolved in 0.5 mL of 5 % D-Mannitol, 0.01 % sodium azide, pH 5.5 at a concentration of 2 mg/mL in the presence of 400 μM LMW heparin (5 kDa heparin, CalBioChem) in 1.5 mL eppendorf tubes and were incubated as described above. For co-aggregation studies, individual peptides were dissolved in 5 % D-mannitol, 0.01 % sodium azide, pH 5.5. Aβ peptides and each of the neuropeptides were mixed at 1:1 ratio and incubated at 37 °C with slight rotation for the fibril formation.

Circular Dichroism Spectroscopy (CD)

10 μL of peptide solution was diluted in 5 % D-mannitol into 200 μL. The peptide solution was placed into a 0.1-cm path-length quartz cell (Hellma, Forest Hills, NY). Spectra were acquired using a JASCO 810 instrument. All measurements were done at 25 °C. Spectra were generally recorded over the wavelength range of 198–260 nm. Three independent experiments were performed with each sample. Raw data

were processed by smoothing and subtraction of buffer spectra, according to the manufacturer's instructions.

Thioflavin T (ThT) Binding

A 5 μL aliquot of peptide sample was diluted to 500 μL in 5 % D-mannitol containing 0.01 % (w/v) sodium azide. The solution was mixed with 2 μL of 1 mM ThT prepared in the same solution. ThT Fluorescence was measured immediately after addition of ThT. The fluorescence experiment was carried out either using Hitachi F-2500 or Horiba-JY (Fluoromax 4), with excitation at 450 nm and emission from 460–500 nm. The intensity values at 480 nm were plotted. For TFE titration studies, the ThT fluorescence of different concentrations of TFE (0–80 %) in water were measured and subtracted from the ThT spectra of respective physalaemin-TFE. A rectangular 10 mm quartz micro-cuvette was used and three independent experiments were performed for each sample.

Tyrosine Fluorescence

A 5 μL aliquot of peptide samples were diluted to 500 μL in 5 % D-mannitol containing 0.01 % (w/v) sodium azide. The fluorescence of Tyr was measured with excitation at 280 nm and emission at 300–500 nm using spectrofluorometer (Hitachi F-2500), in a rectangular 10 mm quartz micro-cuvette.

Acrylamide Quenching

Stock solution (5 M) of acrylamide was prepared in 5 % D-mannitol and stored at 4 °C after filtration by a syringe filter of 0.22 μm (Milipore). Acrylamide was added in increasing concentration (0–500 mM) to the 200 μL of 20 μM solutions of physalaemin and fluorescence spectroscopy was performed immediately. Fluorescence spectroscopy was measured by Hitachi-F2500 fluorescence spectrophotometer by exciting at 280 nm and emission in the range of 290–500 nm using both the excitation and emission slit widths of 5 nm. In each concentration of acrylamide, the fluorescence intensity was corrected by dilution factor of added volume of acrylamide. The fluorescence intensity at 305 nm in absence of any acrylamide was considered as F_0. The fluorescence intensity at 305 nm in the presence of different concentrations of acrylamide was considered as F. At different acrylamide concentrations, F_0/F was calculated and plotted against concentrations of acrylamide.

Congo Red (CR) Binding

A 5 μL aliquot of peptide sample was mixed with 80 μL of PBS buffer containing 10 % ethanol. Then 15 μL of a 100 μM CR solution (filtered through 0.22 μm filter) in PBS containing 10 % ethanol was added. After mixing, absorbance was measured from 400 to 600 nm using Hitachi U-2900 spectrophotometer. For the measurement of the CR-only spectrum, 15 μL of CR solution with 85 μL of PBS containing 10 % ethanol was prepared. As a control, 5 μL aliquot of peptide solutions with 95 μL of PBS containing 10 % ethanol were measured. Three independent experiments were performed for each sample.

Electron Microscopy (EM)

A 5 μL aliquot of peptide sample was diluted in distilled water to a peptide concentration of ~50 μM, spotted on a glow-discharged, carbon-coated Formvar grid (Electron Microscopy Sciences, Fort Washington, PA), incubated for 5 min, washed with distilled water, and then stained with 1 % (w/v) aqueous uranyl formate solution. Uranyl formate solution was freshly prepared and filtered through 0.22 μm sterile syringe filters (Milipore). EM analysis was performed using a FEI Tecnai G^2 12 electron microscope at 120 kV with nominal magnifications in the range of 26,000–60,000. Images were recorded digitally by using the SIS Megaview III imaging system. At least two independent experiments were carried out for each sample.

Atomic Force Microscopy (AFM)

For atomic force microscopy, 2 mg/mL peptide solutions were diluted to 100 fold by water, and diluted sample was spotted on a freshly cleaved mica sheet followed by washing with water. The mica was dried under vacuum desiccators. The imaging was done in tapping mode under a silicon nitride AFM cantilever using Veeco Nanoscope IV multimode AFM. At least five different areas of two independent samples were scanned with a scan rate of 1.5 Hz.

TANGO Analysis

All peptide sequences were subjected to TANGO analysis [30], which predicts the propensity of amyloid aggregation in proteins/peptides. The algorithm is primarily based on simple physico-chemical principles of secondary structure formation and the assumption that aggregating sequence in proteins are fully buried [30]. TANGO was performed at pH 7.0 at 298 K at an ionic strength of 0.02, assuming a protein/peptide stability of −10.

WALTZ Analysis

WALTZ is a web-based tool and uses a position-specific scoring matrix to determine amyloid-forming sequences

[31]. Along with TANGO analysis, all the peptides were also evaluated for their amyloid score by WALTZ calculation. All the predictions were carried out at pH 7.0 with high sensitivity threshold.

MTT Metabolic Assay

The 3-(4,5-dimethylthiazol-2-yl)-2,5-diphenyl tetrazolium bromide (MTT) assay was carried out to evaluate the toxicity of these peptide amyloids compared to Aβ amyloid using neuronal cell line (SH-SY5Y). Cells were cultured in Dulbecco's Modified Eagle Medium (DMEM) (Himedia, India) medium supplemented with 10 % FBS (Invitrogen), 100 U/mL penicillin and 100 μg/mL streptomycin in a 5 % CO_2 humidified environment at 37 °C. Cells were seeded at a density of 10,000 cells per well on 96-well plates in 100 μL medium. After 24 h of incubation, the old culture media was replaced with fresh media containing the test samples and cells were further incubated for 24 h at 37 °C. For co-aggregated samples with Aβ(25–35), the incubation time with cell was 48 h. After incubation, 10 μL of a 5 mg/mL MTT stock in PBS was added to each well and the incubation was continued for 4 h. Finally, 100 μL of a solution containing 50 % dimethylformamide and 20 % SDS (pH 4.7) was added to each well and incubated. After overnight incubation in a 5 % CO_2 humidified environment at 37 °C, absorption values at 560 nm were determined with an automatic microtiter plate reader (Thermo Fisher Scientific).

Neuronal Survival Assay

SH-SY5Y neuron cells were plated in poly-lysine-coated 24 well tissue culture plates at a density of ~10,000 per well in DMEM medium supplemented with 10 % FBS, 100 U/mL penicillin and 100 μg/mL streptomycin. Cells were incubated for 24 h in a 5 % CO_2-humidified environment at 37 °C. After 24 h, the old media was replaced by fresh media containing 10 μM of aged kassinin amyloid fibrils (formed in presence and absence of heparin) and further incubated for 24 h. The number of cell survived in presence of kassinin amyloid was compared with cell treated with similar concentration of Aβ42 amyloid fibrils, which was used as a positive control. 5 % D-mannitol was used in similar dilution as a negative control. The cell viability was assayed using Calcein-AM, fluorescent live/dead stain (Molecular Probes, Invitrogen).

Results

Theoretical Consideration

We were interested in studying whether tachykinin family of peptides can form amyloids as these peptides possess sequence similarity with Aβ(25–35) [19, 28] and stores inside the secretory granules. The amyloidogenic propensities of all the listed peptides (Fig. 1) were calculated using TANGO [30] and WALTZ [31] algorithms. TANGO is a prediction tool, which is developed based on simple physico-chemical principles of secondary structure formation with the assumption that the core regions of an aggregate are fully buried. Whereas WALTZ confers the position-specific amyloid score and can distinguish the amyloid versus amorphous aggregates. WALTZ also more precisely predicts the amyloid-forming potential of functional amyloid sequence containing more polar amino acid residues. All the prediction was carried out at pH 7.0 with high sensitivity threshold. WALTZ prediction inferred that out of three listed peptides, two have sequence with high amyloidogenic score. Physalaemin did not show any amyloid propensity in WALTZ calculation. TANGO algorithm has suggested that Aβ(25–35) have high amount of amyloidogenic propensities whereas none of the peptides under study showed significant amyloidogenic propensities.

Analysis of Aggregation and Amyloid Formation by Neuropeptides

To study the aggregation, conformational transition and amyloid formation by tachykinin peptides, CD, ThT and CR binding were performed at initial (day 0) and final (day 15) days of incubation. All the three peptides were dissolved in 2 mg/mL concentration in 5 % D-mannitol, 0.01 % sodium azide, pH 5.5, and incubated at 37 °C with slight rotation. All peptides were predominantly unstructured immediately after dissolution, as indicated by prominent negative molar ellipticities at ~198 nm (Fig. 2a). The CD studies after 2 weeks of incubation showed significant conformational transition by kassinin; whereas other two peptides remained as mostly unstructured. The ThT binding studies were performed to reveal whether these peptide formed amyloids or not. ThT is a dye, which binds β-sheet-rich amyloids but does not bind to monomeric protein/peptides. When it binds to amyloid, it shows large increase in the fluorescence at 480 nm upon excitation at 450 nm [5]. None of the peptides binds ThT significantly at day 0 and after 2 weeks of incubation (Fig. 2b). Amyloid fibril formations were further measured by CR binding. CR, also routinely used to detect β-sheet-rich amyloid assemblies [4]. CR binding generally measured by the ''red shift'' change of its absorption maximum from 490 to 540 nm and by an increase of the dye's molar absorptivity. None of the peptides bind CR significantly after 15 days of incubation (Fig. 2c). The EM and AFM on 15-days incubated samples were studied to examine the morphology of the samples. Only kassinin showed

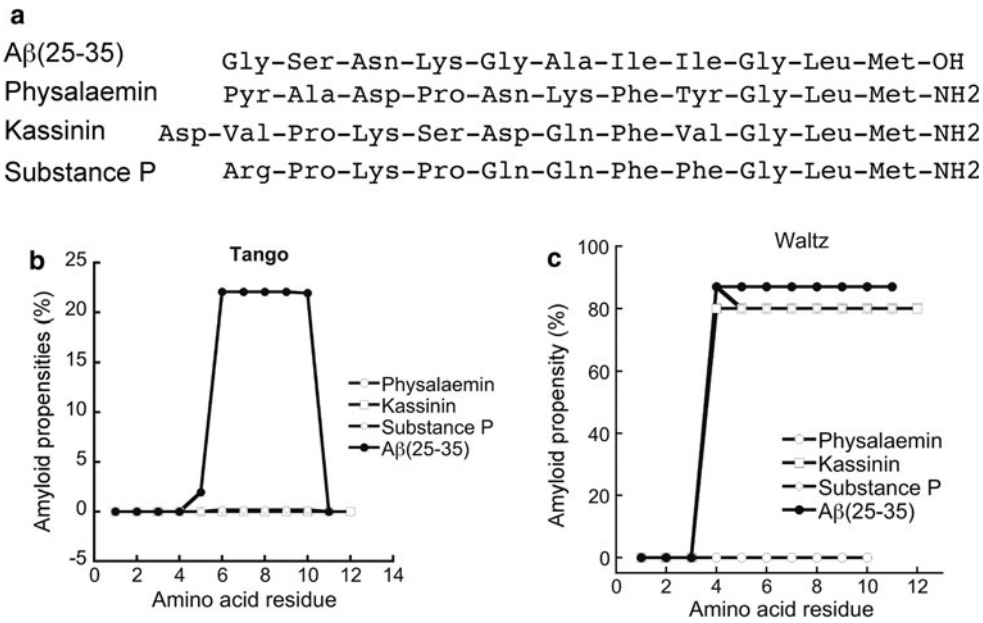

Fig. 1 Comparative analysis of tachykinin neuropeptides and Aβ(25–35). **a** Amino acid sequences of neuropeptides and Aβ(25–35). **b** Aggregation-prone segments of the neuropeptides were predicted by the TANGO and **c** WALTZ algorithms at pH 7.0. Values >0 are indicative of aggregation-prone segments of the peptide sequences

amyloid-like fibrils in solution (Fig. 3), that are consist of non-branched filaments of ~10 nm in diameter and few micrometers long. Few short fibrils were also observed. Individual filaments either helically twisted or laterally associated with each other to form higher order fibrils. Physalaemin and sub-P did not show any fibrils under EM. The AFM study also showed the presence of few non-branched fibrils in 15 days incubated kassinin (Fig. 3); whereas only low order oligomers were seen for physalaemin and sub-P. These data clearly showed that kassinin is able to form amyloids in vitro.

Tachykinin Peptides Formed Amyloid-Like Fibrils in Presence of Heparin

It has been suggested that proteoglycans/glycosaminoglycans (GAGs) play a significant role in amyloid formation and its stability [32–38]. GAGs are associated with amyloid deposits in many human diseases and also play a crucial role in packaging of secretory peptide/proteins into secretory granules [13, 39, 40]. To study whether GAGs can affect the aggregation and amyloid formation by tachykinin family of peptides, the peptides were dissolved in 2 mg/mL concentration in 5 % D-mannitol, 0.01 % sodium azide, pH 5.5, and 400 µM low molecular weight (LMW) heparin was added. The solutions were incubated at 37 °C with slight rotation for 2 weeks. The amyloid formations were studied using CD, ThT, and CR binding and the morphology of the incubated samples was studied using EM and AFM. The CD data showed that immediately after addition of 400 µM heparin, large structural transitions occurred in kassinin and sub-P (Fig. 4a). Kassinin showed CD spectrum with single minima at 225 nm whereas sub-P showed spectrum of two minima, one at 208 and another at 228, closely related to the CD spectra of helical conformation. The CD spectrum of physalaemin did not show significant structural transition and remained mostly unstructured in the presence of heparin. After 2 weeks of incubation, no significant changes in secondary structure were observed for kassinin and sub-P compared to their initial conformation at day 0. However, subtle decrease in helical signal was noticed for sub-P and large increase in positive signal was observed at ~200 nm for kassinin. Physalaemin on the other hand, only showed little decrease in CD signal at ~198 nm consistent with more structure formation during time (Fig. 4a) [41] while maintaining natively unstructured state through out the incubation period. Interestingly, significant ThT binding were observed at day 0 as well as for 15 days incubated samples of kassinin and sub-P indicating amyloid fibrils formation, whereas no ThT binding was observed for physalaemin (Fig. 4b). Similar observation was also obtained from CR binding study of 15-days incubated sample showing significant CR binding by kassinin and sub-P (Fig. 4c), whereas physalaemin did not show any CR binding. The EM and AFM data (Fig. 5) showed the densely packed amyloid fibrils formed by kassinin and long filaments of ~10 nm in diameter formed by sub-P. Physalaemin showed thin and short fibrils both under EM and AFM after 15 days of incubation. The data have suggested that all three peptides posses amyloidogenic potential; however, physalaemin is less amyloidogenic compared to other two peptides.

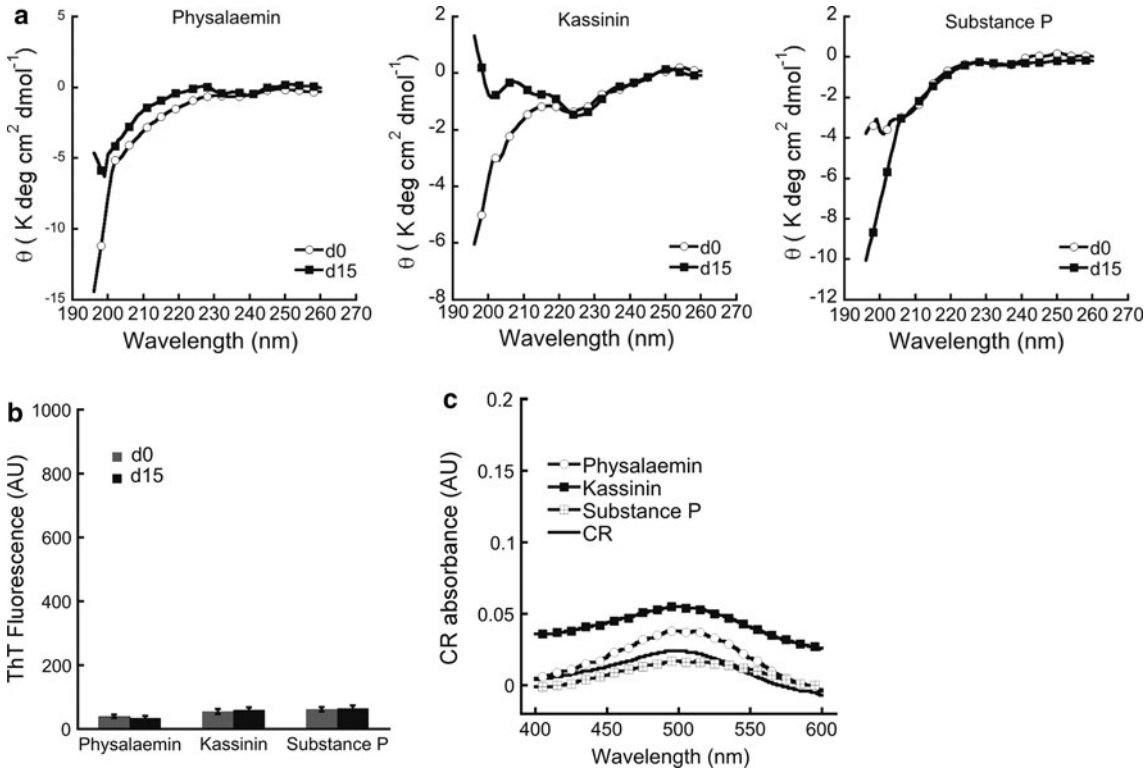

Fig. 2 Aggregation and amyloid formation of neuropeptides in vitro. Peptides at a concentration of 2 mg/mL in 5 % D-mannitol were incubated with slight agitation at 37 °C for 15 days. **a** CD spectra of samples at day 0 and day 15. Only kassinin showed significant structural transition after 15 days of incubation. **b** ThT binding of the peptides. None of the peptide binds ThT significantly at day 0 and day 15 indicating absence of amyloids. **c** CR absorbance between 400 and 600 nm showing no significant increment of molar absorptivity as well as the absence of "red shift" of its absorption maximum at 490 nm indicating the absence of any amyloid formation

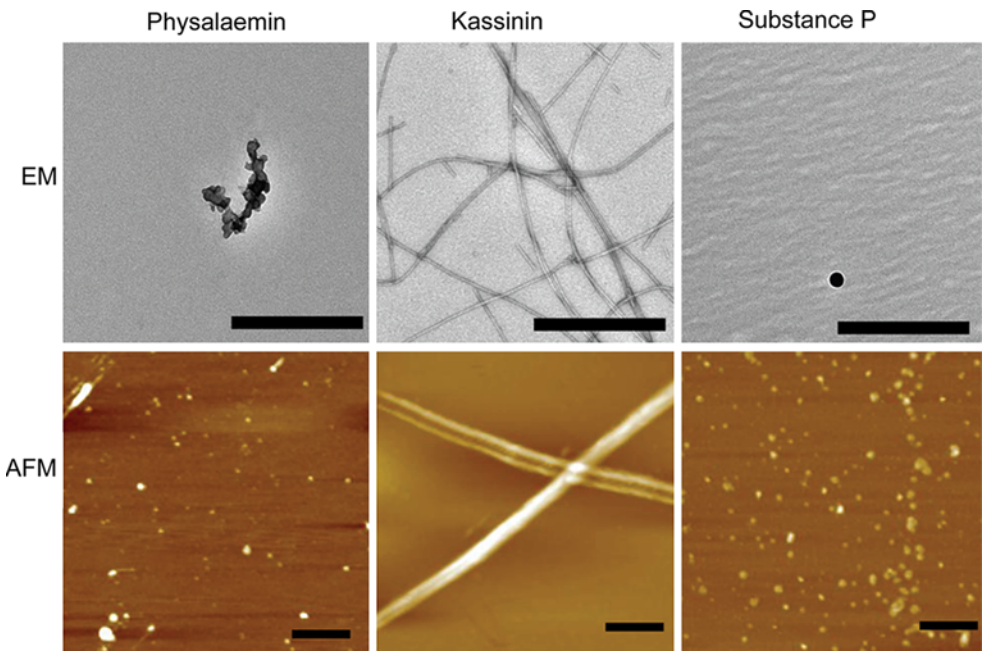

Fig. 3 Morphology of neuropeptide aggregates. EM and AFM were performed with the 15-days incubated samples. Only kassinin showed the formation of amyloid-like fibrils. *Scale bars* are 500 nm

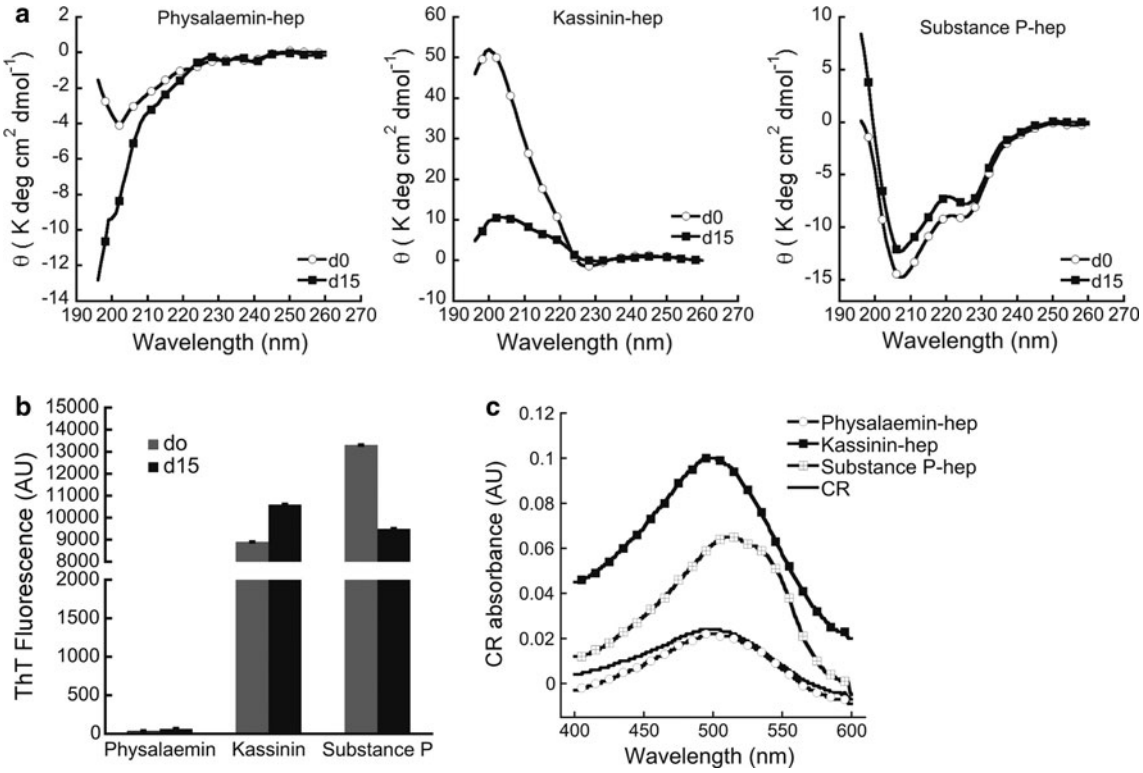

Fig. 4 Amyloid formation by neuropeptides in the presence of heparin in vitro. 2 mg/mL solution of each peptide was incubated in presence of 400 μM heparin prepared in same solution. **a** Conformational transition of peptides during incubation by CD spectroscopy. Immediate after addition of heparin both kassinin and sub-P showed significant structural transition. The structure of these peptides remained mostly unaltered after 15 days of incubation. Physalaemin remained mostly unstructured at day 0 as well as day 15. However, reduced intensity at 198 nm was observed suggesting some structure formation during incubation. **b** ThT binding of peptides suggesting that both kassinin and sub-P bind significant amount of ThT suggesting their amyloid formation. Physalaemin did not show any ThT binding. **c** CR absorbance between 400 and 600 nm showing increased absorbance and the "red shift" of its absorption maximum from 490 nm suggesting the presence of amyloid for kassinin and sub-P. Physalaemin did not show any significant CR binding

Changes in Tyr Microenvironment in Physalaemin Aggregation

The aggregation data suggested that physalaemin neither show any significant structural transition in CD nor able to bind ThT and CR. However, it showed amyloid fibrils in presence of heparin observed under EM and AFM. It is important to note that EM and AFM are capable of showing amyloids even if only minority of the peptide samples formed amyloid. These data suggest that there might be subtle structural changes in physalaemin occurred during incubation. This structural change might not be visible in CD, as it is conformation-averaging technique and only major conformation could be observed. Since, physalaemin contains a single Tyr at position 8, we decided to study the Tyr intrinsic fluorescence [41, 42] to show whether amyloid fibril formation is accompanied by changes in Tyr microenvironments. The one Phe residue at position 7 is fluorometrically silent because of its low quantum yield and therefore, Tyr^8 could provide a suitable probe for structural transition. Tyr fluorescence was performed at day 0 and day 15 and the data showed that fluorescence intensity of physalaemin was increased after 15 days of incubation, suggesting that Tyr microenvironment have changed during incubation (Fig. S1A). The increment of Tyr fluorescence intensity was greatly enhanced by the addition of heparin (Fig. S1B). The fluorescence intensity after 2 weeks of incubation was almost double suggesting that significant change in Tyr microenvironment occurred in physalaemin in the presence of heparin. We suggest that Tyr in aggregated state of physalaemin is less solvent-exposed and therefore increment of Tyr fluorescence might have observed. To examine the solvent exposure of Tyr, acrylamide quenching of 15 days incubated physalaemin samples were performed. The data suggest that the Tyr in 15-days aged sample incubated in the presence of heparin is less solvent-exposed compared to physalaemin incubated in the absence of heparin (Fig. S1C). The upward curve of Stern–Volmer plot in physalaemin in the absence of heparin has suggested that both static and dynamic quenching might have occurred [42]. Our data clearly indicate that small structural transition and large change of Tyr

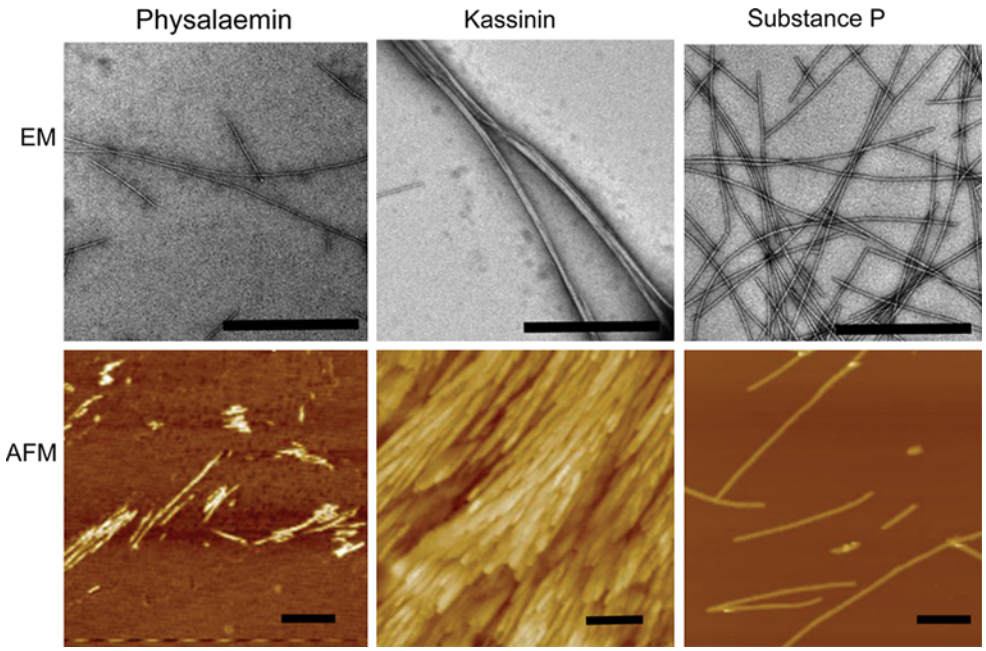

Fig. 5 Morphology of peptide aggregates in the presence of heparin. EM and AFM were performed with 15-days incubated peptides in the presence of heparin. All three peptides showed amyloid-like fibrillar morphology in the presence of heparin. Scale bars are 500 nm

microenvironment might accompany the physalaemin fibril formation.

Modulation of Secondary Structure and Fibril Formation of Physalaemin by Cosolvent TFE

2,2,2-Trifluoroethanol (TFE) is known to destabilize hydrophobic interaction within the polypeptide chain and stabilizes local hydrogen bonds between residues close in the amino acid sequence [43]. TFE is well known organic solvent to induce and stabilize helices in peptide/proteins. Previously many studies have suggested that intermediate concentrations of TFE can induce amyloid formation in peptide and proteins [44–46]. Since physalaemin did not show significant structural transition and amyloid formation, we decided to analyze its amyloid formation tendency in TFE. To study the effect of TFE on the secondary structure propensity and assembly reaction, TFE titration was performed where increasing concentration of TFE (0–80 %) was added to freshly prepared monomeric physalaemin (Fig. S2). Immediately after TFE addition, CD and ThT fluorescence were measured. Our data showed that significant amount of helicity was induced by addition of increasing amount of TFE (Fig. S2A). The ThT binding studies in moderate TFE concentrations (20–50 %) clearly indicates that favoring partial folding (helix induction) might accelerate amyloid formation (Fig. S2B). Interestingly, partial helix induction promotes amyloid formation by Aβ and other amyloidogenic peptides [44–46]. Physalaemin samples in varying concentration of TFE (0–80 % (v/v)) were further incubated at room temperature for 7 days to evaluate fibril assembly. CD data suggest that physalaemin did not undergo further structural transition to β-sheet conformation (Fig. S2C). Interestingly, AFM data of incubated sample in 30 % TFE showed numerous amyloid-like fibrils (Fig. S2D). The data clearly indicates that physalaemin is capable of amyloid formation in presence of intermediate concentrations of TFE with major helical conformation.

Amyloids of Tachykinin Peptides are Nontoxic In Vitro

Amyloid fibrils are considered as toxic species as they are associated with several human disorders [1]. Furthermore, amyloids formed by several protein/peptide in vitro have shown to be cytotoxic in nature. Recent studies have suggested that oligomers formed in the pathways of amyloid formation are more cytotoxic compared to mature amyloids [47–50]. Previous studies have suggested that cytotoxicity of amyloids could depend on the primary structure of protein/peptides and the nature of surface of the amyloids [2]. To evaluate the toxicity of amyloid formed by tachykinin peptides, MTT assay [51] was carried out with SH-SY5Y cell line. The cellular toxicity was also performed for Aβ42 amyloid fibrils as a positive control (Fig. 6). In the presence of 10-μM Aβ42 fibrils, MTT reduction was decreased to 57 %. In contrast, all the three tachykinin peptides either in non-aggregated or in amyloid state (10 μM) did not decrease

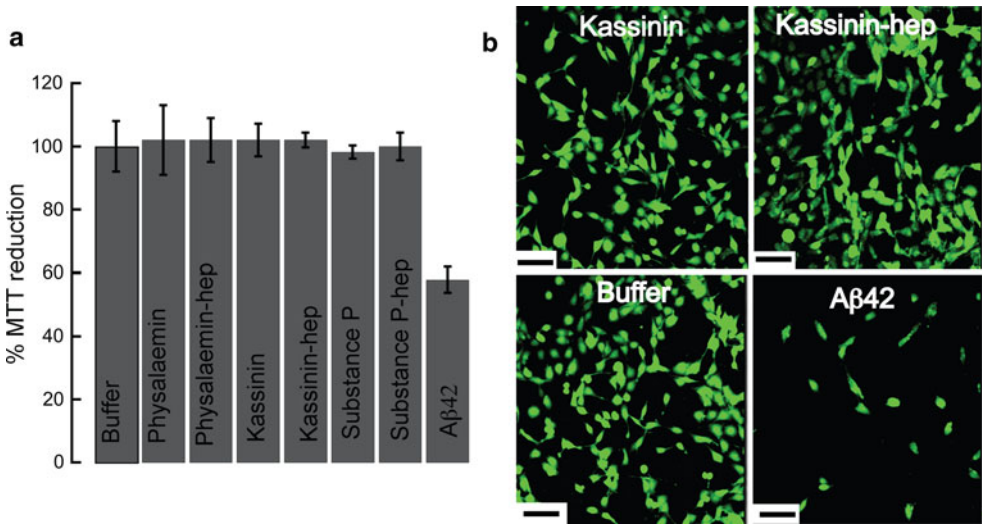

Fig. 6 Toxicity of peptide aggregates. **a** MTT reduction by the SH-SY5Y cell line in presence of peptide samples (10 μM) were measured with respect to buffer. Aβ42 fibrils were used as positive control. All peptides were incubated under slight agitation for 15 days at 37 °C at concentrations of 2 mg/mL in absence and presence of 400 μM LMW heparin. Only Aβ42 showed significant reduction of MTT. The data suggesting amyloid of neuropeptides are nontoxic in nature. **b** The survival of SH-SY5Y neuronal cell were measured after 1-day exposure of 15 days old kassinin fibrils prepared in presence and absence of heparin. Fluorescence microscopy showing the viable cells that labeled with the fluorescence dye Calcein (Molecular Probes, Invitrogen). Only Aβ42 significantly reduced the number of viable cells under study

MTT reduction considerably compared to buffer control. To further support the observation, the survival of SH-SY5Y cells was measured following the addition of amyloid fibrils of kassinin and Aβ42 [13]. Kassinin was selected since this peptide was able to form amyloid both in the presence and absence of heparin. More number of cells survived in the presence of kassinin fibrils compared to Aβ42 fibrils. Therefore, the MTT and neuronal survival assays indicate that these neuropeptide amyloids are nontoxic.

Co-aggregation of Aβ(25–35) and Tachykinin Neuropeptides

To evaluate whether tachykinin neuropeptides are able to co-aggregate with Aβ(25–35) peptide for amyloid fibril formation, Aβ(25–35), sub-P and kassinin peptides were dissolved in 5 % D-mannitol, 0.01 % sodium azide, pH 5.5 at a concentration of 2 mg/mL. 800 μM solution of each of sub-P and kassinin were added to 800 μM of Aβ(25–35) so that the final concentration of each peptide in the mixture was 400 μM. To induce the aggregation process 400 μM LMW heparin was also added to these solutions. As a control, 400 μM each of Aβ(25–35), sub-P and kassinin were also prepared and incubated in the presence of 400 μM LMW heparin. All these peptide solutions were incubated at 37 °C with slight agitation. The ThT fluorescence and CD were performed at day 0. After 1 day of incubation at 37 °C with slight agitation, ThT and EM were also performed. At day 0, Aβ(25–35) showed significantly high ThT binding suggesting substantial amount of amyloid formation (Fig. 7a). ThT fluorescence was ~1.5 fold higher when Aβ(25–35) was mixed with sub-P compared to the combined ThT binding value of Aβ(25–35) and sub-P. Sub-P alone in the presence of heparin did not show significant ThT binding at day 0. However, after 1 day of incubation, sub-P in the presence of heparin showed significant increase in ThT binding whereas the ThT binding of the mixture of Aβ(25–35) and sub-P in the presence of heparin did not increase significantly. Moreover, after 1-day incubation, Aβ(25–35) showed little decrease in ThT binding compared to day 0 suggesting precipitation and/or lateral association of fibrils with lower ThT binding sites. In contrast to the co-aggregation of Aβ(25–35)–sub-P, there was no significant increase in net ThT binding of the Aβ(25–35)–kassinin mixture in presence of heparin compared to the combined ThT binding value of Aβ(25–35) and kassinin.

The effect of secondary structure due to the co-aggregation was further studied by CD spectroscopy at day 0. The data (Fig. 7b) suggested that β-sheet-rich amyloid formation of Aβ(25–35) as CD spectrum showed single minima ~218 nm. Interestingly, when Aβ(25–35) was mixed each with sub-P and kassinin, significantly different CD spectra were observed. The mixture of Aβ(25–35) and sub-P showed CD spectrum with two minima; one at

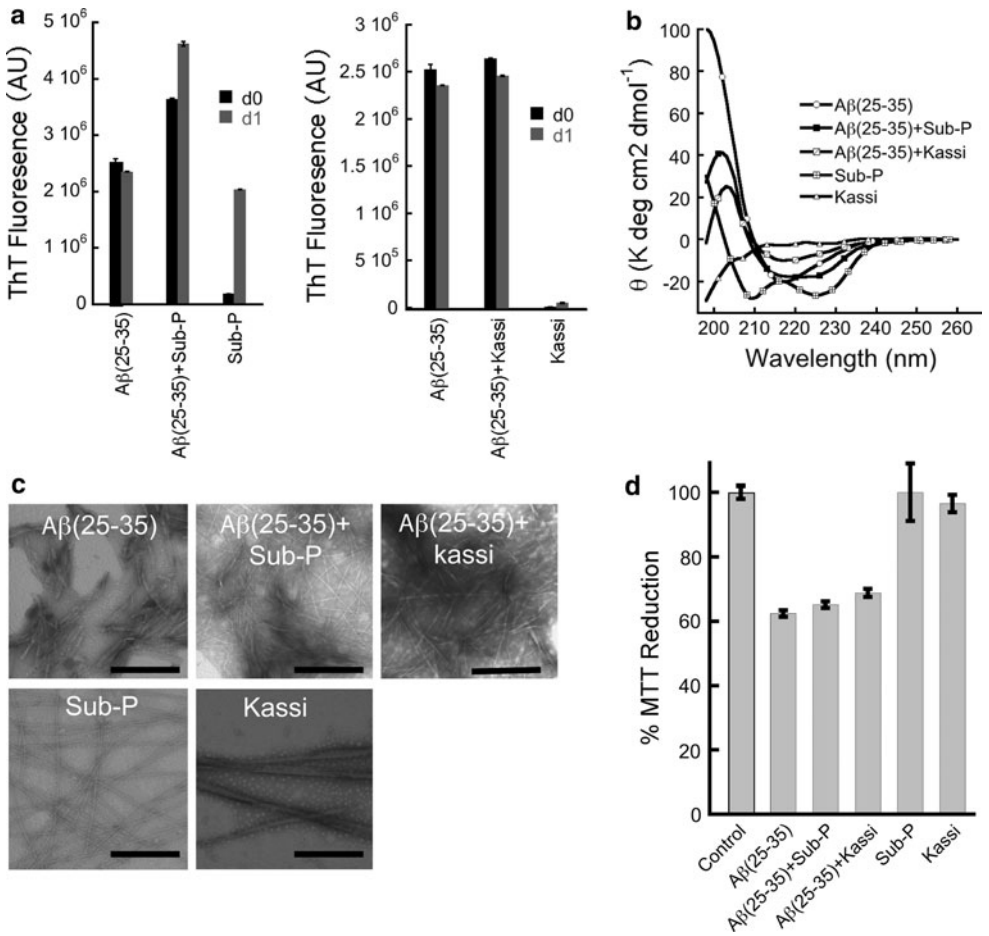

Fig. 7 Co-aggregation studies of Aβ(25–35) and tachykinin peptides in vitro. **a** Aβ(25–35) solution was mixed each of sub-P and kassinin (kassi) in 1;1 ratio where final concentration of each peptide was 400 μM. These peptides were incubated at 37 °C with slight agitation in presence of 400 μM LMW heparin. ThT was performed at day 0 (d0) and after 1 day of incubation (d1) and EM were performed at day 1. CD was performed at d0 to reveal the secondary structural changes due to co-aggregation. Significantly higher ThT binding was observed for fibrils formed by the mixture of Aβ(25–35) and sub-P. **b** Aβ(25–35) in presence of equimolar concentration of either kassinin and sub-P showed altered CD spectrum at day 0 suggesting interaction between Aβ(25–35) and neuropeptides. **c** The EM study suggesting that morphology of the mixed sample of Aβ(25–35)–kassi and Aβ(25–35)–Sub-P were different than that of Aβ(25–35), kassinin, and sub-P alone after 1 day of incubation. *Scale bars* are 500 nm. **d** The MTT assay of mixed sample containing 20 μM Aβ(25–35) and 20 μM tachykinin peptide showed comparatively higher MTT reduction in SH-SY5Ycells compared to 20 μM Aβ(25–35), suggesting the increased cell viability in the presence of tachykinin neuropeptides. Sub-P and kassinin alone were found to be nontoxic

217 nm and other at 226 nm, suggesting alteration of secondary structure of the mixed fibrils. The mixture of Aβ(25–35) and kassinin showed a CD spectrum with single minima ~218 nm, suggesting β-sheet-rich amyloid. However, decrease in CD intensity at ~218 nm suggesting lesser content of β-sheet in amyloid fibrils. The EM image of 1 day incubated samples of Aβ(25–35) showed formation of very short fibrils ranging from ~200–700 nm in length and ~20–40 nm in diameter (Fig. 7c). Several thin protofilaments were laterally associated and/or helically twisted to form these fibrils. Interestingly, morphology of fibrils formed by 1:1 mixture of Aβ(25–35) and sub-P showed mostly long and thin fibrils of ~10–25 nm in diameter. The fibrils formed by the mixture of Aβ(25–35) and kassinin showed long fibrils formed by many thin protofilaments. In contrast, solution containing only sub-P formed very thin, straight, and long filaments of ~10–15 nm in diameter and kassinin showed ~30–80 nm diameter fibrils composed of numerous protofilaments.

The ThT, CD, and EM data strongly suggested that Aβ(25–35) and tachykinin peptides such as sub-P and kassinin may co-aggregate to form distinct amyloid fibrils. To evaluate the cytotoxicity of the co-aggregates formed by Aβ(25–35)–sub-P and Aβ(25–35)–kassinin, the samples were tested by MTT assay (Fig. 7d). One-day incubated samples of 20-μM Aβ(25–35), mixed aggregates of 20-μM Aβ(25–35) and 20 μM either of sub-P and kassinin were incubated with SH-SY5Y cells for 48 h in 96 well plates.

MTT assay was performed and the data revealed that slight increases in MTT reduction with co-aggregated samples (Fig. 7d).

Tachykinin Neuropeptides Co-aggregate with Aβ40 into Morphologically Different Amyloid Fibrils

To evaluate the synergistic effect of tachykinin and Aβ40 peptides on their aggregation, we performed aggregation study of Aβ40 in the presence and absence of equimolar concentrations of each tachykinin peptide in vitro. 400 μM each of tachykinin peptides were diluted with 400 μM of Aβ40 peptide and the final concentrations of each peptide in the mixture was 200 μM. For control study, 200 μM of Aβ40 and each of tachykinin peptides alone were used. All the peptide solutions were incubated at 37 °C with slight agitation for 1 week and amyloid aggregation was quantified by ThT binding assay both at day 0 and after 1 week of incubation (Fig. 8). Insignificant ThT binding for all the tachykinins alone were seen at day 0. Whereas Aβ40 alone showed relatively high ThT suggesting that this peptide is more amyloidogenic compared to any of the tachykinin peptides in absence of heparin. Although, the mixture of Aβ40 and physalaemin did not show any significant difference in ThT binding compared to Aβ40 alone at day 0, the mixture of Aβ40-sub-P and Aβ40-kassinin showed high ThT binding compared to the combined ThT binding value of Aβ40 and each of sub-P and kassinin peptides (Fig. 8a). Interestingly after 1 week of incubation, ThT fluorescence intensity of Aβ40-tachykinin mixed samples increased significantly compared to that of Aβ and tachykinin alone. ThT binding of 1 week incubated samples of Aβ-kassinin mixture showed maximum increase (∼fourfold) followed by Aβ40-sub-P (∼twofold) and Aβ40-physalaemin mixture (∼1.5-fold) compared to 1 week incubated Aβ alone sample. The data suggests that the synergistic aggregation of Aβ40 and each of tachykinins occurred in mixed samples. The morphological characterization of 1 week incubated samples using EM showed significant difference in the morphology of the mixed aggregates compared to the individual aggregates (Fig. 8b). One week incubated Aβ sample showed few thin fibrils as well as small oligomeric aggregates, whereas physalaemin, sub-P, and kassinin showed mostly amorphous-like aggregates. Interestingly, all Aβ-tachykinin mixed samples showed dense population of highly ordered fibrillar aggregates with distinct morphology compared to Aβ fibrils after 1 week of incubation. Aβ40-physalaemin showed networks of numerous long fibrils that were composed of 2–3 individual filaments. The diameter of these fibrils was ∼10–15 nm. The EM image of the Aβ40-sub-P mixture also showed highly clustered fibrillar aggregates. The Aβ40-kassinin mixture formed long fibrils made by multiple filaments that were either helically twisted or parallel associated with each other. The diameter of these fibrils was of ∼20–30 nm (Fig. 8b).

Kassinin Amyloid Accelerates the Aggregation of Aβ40 Peptide by Cross-Seeding

Amyloid formation by protein/peptide is a nucleation dependent polymerization process [52]. Therefore, in the presence of minute amount of preformed amyloid seeds, the kinetics of amyloid formation in protein is accelerated. However, seeding requires a high amino acid sequence similarity between the protein/peptide of the seed and its soluble host protein [1, 53]. Amyloid seeds from one protein/peptide can also accelerate the amyloid formation by other protein and this phenomenon is called "cross-seeding" [54]. Previously cross-seeding between different proteins species have been documented in human diseases [54]. To study the seeding effect of kassinin fibrils with Aβ40, kassinin seeds were prepared by sonicating 1 mM solution of 1-month aged kassinin fibrils for 30 min in bath sonicator at room temperature. The sonicated kassinin fibrils were then added at a concentration of 1, 5 and 10 % (v/v) to 200 μM freshly prepared Aβ40 solution in 5 % D-mannitol, 0.01 % sodium azide, pH 5.5. The samples were incubated at 37 °C with slight rotation and the aggregation was monitored by ThT fluorescence at regular intervals. The ThT fluorescence values at 480 nm were plotted against incubation time (Fig. 9a). After 10 days of incubation EM was performed with all incubated samples (Fig. 9b).

The data suggested that 1–5 % seeds of kassinin fibrils did not altered the lag phase of the Aβ40 aggregation kinetics. However, little increase in amyloid formation was observed in kassinin seeded Aβ40 aggregation. In contrast, both accelerated kinetics and higher amount of amyloid fibrils by Aβ40 were observed with 10 % kassinin seeds (Fig. 9a). However, only seeds did not show any significant ThT binding during entire period of incubation (data not shown). The EM study of 10-days incubated samples showed that Aβ40 formed fibrillar aggregates (Fig. 9b). Some small oligomers also were observed. The EM of Aβ40 in presence of 1 and 5 % kassinin seed did not show any significant morphological differences compared to Aβ40 alone after 10 days of incubation. However, numerous thin fibrils were formed in Aβ40 samples seeded with 10 % kassinin fibrils suggesting higher concentration of kassinin amyloid seeds may affect the amyloidogenesis of Aβ40 (Fig. 9b).

Preformed Tachykinin Amyloid Fibrils Reduce the Toxicity of Aβ40 Amyloids In Vitro

To evaluate the effect of tachykinin fibrils on the cytotoxicity of Aβ fibrils, preformed kassinin amyloid fibrils were chosen for the study as kassinin formed amyloid

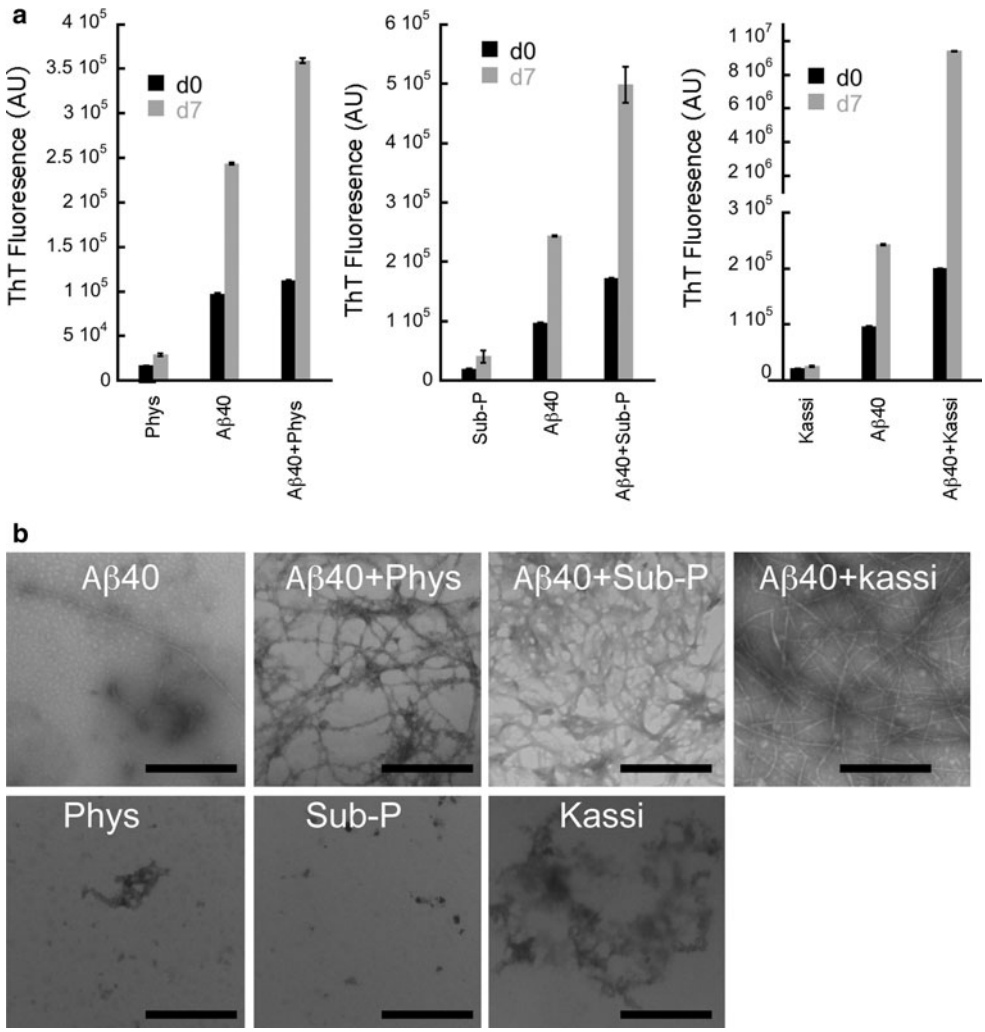

Fig. 8 Co-aggregation studies of Aβ40 with tachykinin peptides in vitro. **a** The 1:1 mixture of Aβ40 and each of tachykinin peptides in 5 % D-mannitol, 0.01 % NaN_3, pH 5.5 were incubated at 37 °C with slight rotation. The final concentration of each peptide was 200 μM in the mixture. 200 μM each of tachykinin peptides and Aβ40 were also incubated in similar conditions for the control. ThT and EM were performed to analyze the co-aggregation. ThT fluorescence at 480 nm for d0 and d7 samples. At day 0 (d0), the 1:1 mixture of Aβ40–sub-P and Aβ40–kassi showed much higher ThT binding compared to the combined ThT value of each peptides. The ThT fluorescence was further increased after 1 week of incubation suggesting the co-aggregation occurred between Aβ40 and each of these neuropeptides. **b** EM study of the aggregates after 1 week of incubation. Aβ40 formed mixture of fibrillar and oligomeric species whereas each of the tachykinin peptides formed amorphous-like aggregates. However, mostly fibrillar morphology distinct from Aβ40 fibrils was seen for mixed samples. *Scale bars* are 500 nm

fibrils both in the absence and presence of LMW heparin and possess large structural transition of random coil to β-sheet during amyloid formation. 10 μM Aβ40 solutions in presence of different concentrations of kassinin fibrils were studied for MTT assay where the molar ratio of Aβ40:kassinin were 1:1, 1:2 and 1:3. After 30 min of incubation at room temperature, these solutions were added to 96-well plates containing SH-SY5Y cells in media. MTT assay was performed with these fibrils mixture after 24 h of incubation with the cells. The MTT data (Fig. 9c) showed that kassinin fibrils were able to reduce toxicity of Aβ40 fibrils in a concentration dependent manner. 10 μM Aβ40 fibrils showed 50 % MTT reduction, whereas ~70 % MTT reduction was seen for 1:1 Aβ40:kassinin fibrils. MTT reduction was ~80 % when Aβ40-kassinin was used in 1:3 ratio (Fig. 9c). These results suggest the possibility that kassinin fibrils may interacts with Aβ and neutralize its toxic epitopes. The crowding at the cell membrane by kassinin fibrils may also reduce the membrane interactions by Aβ amyloids.

Discussion

The discovery of new peptide/proteins with amyloid forming capabilities are important as it could provide not

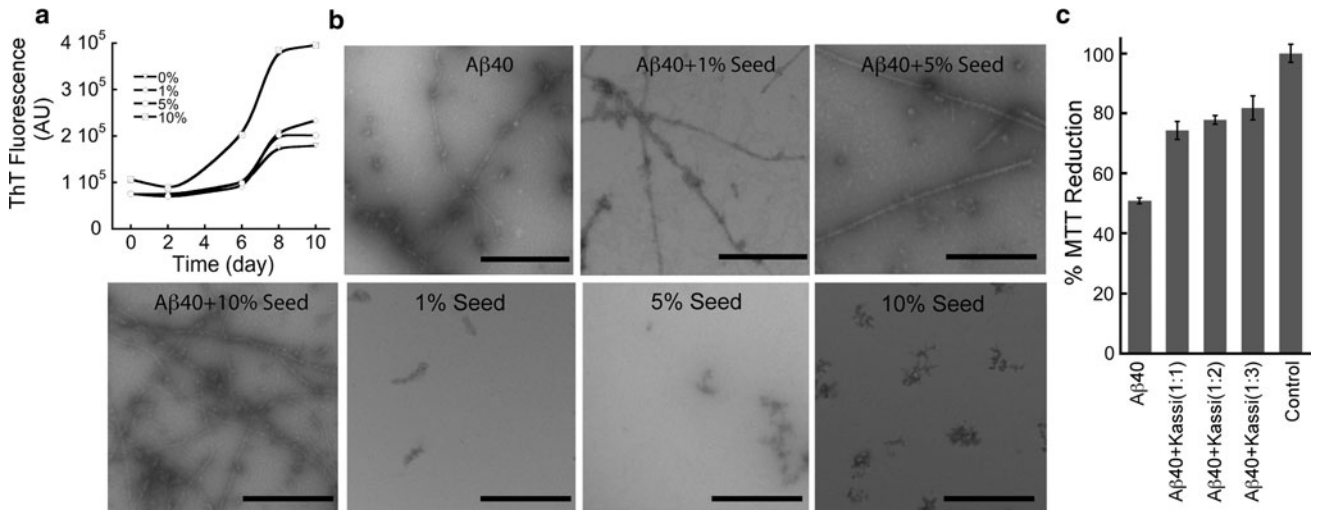

Fig. 9 Cross-seeding of Aβ40 monomer with kassinin amyloid fibrils. **a** The preformed kassinin fibrils were sonicated for 30 min and added to the freshly prepared Aβ40 solution in 5 % D-mannitol, 0.01 % sodium azide, pH 5.5. The final concentrations of seeds were 1 % (v/v), 5 % (v/v), and 10 % (v/v). The Aβ40 solutions in the absence and presence of different concentration of kassinin seeds were incubated at 37 °C with slight rotation. ThT fluorescence was measured at regular interval. After 10 days of incubation EM was performed to determine morphology of the aggregates. Kinetics of the aggregation measured by ThT suggesting significant decrease in lag time and increase in amyloid fibrils for Aβ40 aggregation in the presence of 10 % kassinin seeds. 1 and 5 % seeds did not show any significant change in Aβ40 aggregation kinetics. **b** Electron micrographs showing fibrils formation of Aβ40 in presence of different concentration of kassinin seeds. The data suggest more amount of amyloid formation in presence 10 % kassinin seeds. The morphology of the different concentration of seeds used for the study is also shown. *Scale bars* are 500 nm. **c** MTT reduction of 10 μM Aβ40 fibrils with and without different concentration of kassinin amyloid fibrils. Increased MTT reduction in SH-SY5Y cells with increasing concentration of kassinin fibrils were observed

only a model system to study amyloid aggregation associated with pathogenesis but also could be useful in designing amyloid-based biomaterials [14, 15, 55]. Here, we studied in vitro aggregation and amyloid formation by tachykinin family of neuropeptides in the presence and absence of heparin. All these neuropeptides under study have sequence similarity with Aβ(25–35), which is known to form neurotoxic amyloids similar to the full-length Aβ. Although amyloid-predicting algorithm TANGO failed to show any amyloidogenicity of these three peptides, WALTZ showed the amyloidogenic regions of kassinin and sub-P, when calculated with high sensitivity score (Fig. 1). The data suggest that either WALTZ may over-predicts or TANGO may under-predicts the amyloid-forming capability of protein/peptides. In our independent test with seven different peptide hormones, known to form amyloids in vitro, also failed to show any amyloid sequence in TANGO; whereas all of them showed amyloid tendency when analyzed in WALTZ (Table S1). The data clearly indicates that TANGO under-predicts the amyloid formation of protein/peptides compared to WALTZ. To further confirm the amyloid propensities of these neuropeptides, we tested these peptide sequences with different amyloid-predicting algorithms [56] (Table S2). These algorithms mostly predicted that these peptides possess significant amyloidogenic potential.

Consistent with significant hydrophobicity (Kyte Doolittle scale [57]) and β-sheet propensities (Chou–Fasman scale [58]) at the C-terminus of these neuropeptides along with amyloid prediction by WALTZ algorithm (Fig. 1), all the peptides formed amyloids in vitro after 2 weeks of incubation in the presence of heparin as evident from EM and high ThT binding data (Figs. 4 and 5). The amyloid formation by kassinin and sub-P were accompanied by large structural transition even at day 0 in presence of LMW heparin. Previously, heparin has been shown to accelerate the structural transition and amyloid formation of many proteins/peptides associated with diseases as well as functions [13, 32, 59–62]. The data suggest that although these peptides may possess amyloid forming propensities as predicted from amyloid algorithms, however, negatively charged heparin might be required for their amyloid transformation effectively. The aggregation of physalaemin in presence of heparin showed formation of amyloids under EM/AFM without large structural transition in CD, ThT binding and CR binding (Figs. 4 and 5). The data indicates that small fractions of peptides might have formed amyloid fibrils. Similar results also were found for kassinin aggregation in absence of heparin as EM/AFM study showed the formation of amyloid fibrils without showing any ThT and CR binding. However, this amyloid formation by kassinin was accompanied by large structural transition of random coil to β-sheet.

Amyloid fibril formation by sub-P in our study is intriguing that it showed all the properties of amyloids (high CR and ThT binding, fibrillar morphology under EM/AFM) without formation of β-sheet structure in CD. This peptide formed amyloids with mostly α-helix-rich conformation. Amyloid fibrils of helical conformation are previously reported for tau protein and Neuromedin K associated with Alzheimer's disease and hormone storage [13, 63], respectively. The heparin backbone conformation and its nature of interactions with sub-P may also help to adopt the helical conformation by sub-P amyloid fibrils.

Our data further indicates that although significant sequence similarity may exist among tachykinin peptides, the effect of heparin on the amyloid formation of tachykinin peptides were different. For example, large bundling of amyloids was appeared for kassinin under EM/AFM whereas sub-P showed mostly thin filaments in the presence of heparin (Fig. 5). The physalaemin on the other hand showed few thin fibrils. However, in the presence of moderate concentrations of TFE, physalaemin showed partial helix induction, which converted to amyloid-like fibrils after 7 days of incubation without further structural conversion to β-sheet (Fig. S2). The data indicates that TFE might have induced the aggregation of this peptide into an α-helix-rich intermediates that possess significant amyloid characteristics such as high ThT binding and fibrillar morphology under AFM. However, this intermediate could be off-pathway, which is unable to undergo further β-sheet-rich conformation [64, 65]. Previously, many amyloidogenic peptides showed accelerated amyloid formation when incubated with moderate concentration of TFE—a chemical milieu for partial helix formation of protein/peptides [44, 45].

The co-aggregation study suggests that these neuropeptides co-assemble with Aβ(25–35)/Aβ40 and form higher order amyloid fibrils with accelerated kinetics (Figs. 7 and 8). Furthermore, the cross-seeding ability of kassinin fibrils to the kinetics of Aβ fibril formation suggest that these neuropeptide fibrils may modulate the toxic aggregation pathway of Aβ associated with Alzheimer's disease (Fig. 9). This hypothesis was further strengthened by the observation that co-aggregates of Aβ and tachykinin peptides showed reduced toxicity in SH-SY5Y cells. Furthermore the toxicity of Aβ40 fibrils were reduced when it was diluted with fibrils containing neuropeptide kassinin than that of Aβ40 fibrils diluted with buffer (Fig. 9) suggesting that kassinin fibrils might have sequestered the toxic epitope of Aβ40 amyloids.

The present study not only will help to understand amyloidogenesis of peptide/protein in general, but may also suggest the possible explanation of toxicity reduction of Aβ40 by tachykinin peptides.

Acknowledgments Authors wish to acknowledge IRCC (IIT Bombay), CSIR (37(1404)/10/EMR-11) and DST (SR/FR/LS-032/2009), Government of India for financial supports and Central SPM Facility (IRCC, IIT Bombay) for AFM imaging and SAIF (IIT Bombay) for electron microscopy. We thank Reeba S. Jacob, Shruti Sahay and A. Anoop for critical reading of the manuscript. We are also thankful to Prof. G. Krishnamoorthy (TIFR, Mumbai) and Mr. Prem Verma (Department of Physics, IIT Bombay) for their valuable help during AFM imaging.

References

1. Chiti, F., & Dobson, C. M. (2006). Protein misfolding, functional amyloid, and human disease. *Annual Review of Biochemistry, 75*, 333–366.
2. Maji, S. K., Wang, L., Greenwald, J., & Riek, R. (2009). Structure–activity relationship of amyloid fibrils. *FEBS Letters, 583*, 2610–2617.
3. Tycko, R. (2006). Molecular structure of amyloid fibrils: Insights from solid-state NMR. *Quarterly Reviews of Biophysics, 39*, 1–55.
4. Klunk, W. E., Jacob, R. F., & Mason, R. P. (1999). Quantifying amyloid by Congo red spectral shift assay. *Methods in Enzymology, 309*, 285–305.
5. LeVine, H. (1999). Quantification of β-sheet amyloid fibril structures with thioflavin T. *Methods in Enzymology, 309*, 274–284.
6. Sunde, M., & Blake, C. (1997). The structure of amyloid fibrils by electron microscopy and X-ray diffraction. *Advances in Protein Chemistry, 50*, 123–159.
7. Sunde, M., Serpell, L. C., Bartlam, M., Fraser, P. E., Pepys, M. B., & Blake, C. C. (1997). Common core structure of amyloid fibrils by synchrotron X-ray diffraction. *Journal of Molecular Biology, 273*, 729–739.
8. Dobson, C. M. (1999). Protein misfolding, evolution and disease. *Trends in Biochemical Sciences, 24*, 329–332.
9. Huff, M. E., Balch, W. E., & Kelly, J. W. (2003). Pathological and functional amyloid formation orchestrated by the secretory pathway. *Current Opinion in Structural Biology, 13*, 674–682.
10. Fowler, D. M., Koulov, A. V., Alory-Jost, C., Marks, M. S., Balch, W. E., & Kelly, J. W. (2006). Functional amyloid formation within mammalian tissue. *PLoS Biology, 4*, e6.
11. Fowler, D. M., Koulov, A. V., Balch, W. E., & Kelly, J. W. (2007). Functional amyloid–from bacteria to humans. *Trends in Biochemical Sciences, 32*, 217–224.
12. Jacob, R., Anoop, A., Singh, P., & Maji, S. (2010). Native Functions of Amyloid. In D. A. Stein (Ed.), *Protein aggregation* (pp. 79–109). New York: Nova Science Publishers, Inc.
13. Maji, S. K., Perrin, M. H., Sawaya, M. R., Jessberger, S., Vadodaria, K., Rissman, R. A., et al. (2009). Functional amyloids as natural storage of peptide hormones in pituitary secretory granules. *Science, 325*, 328–332.
14. Mankar, S., Anoop, A., Sen, S., & Maji, S. K. (2011). Nanomaterials: Amyloids reflect their brighter side. *Nano Reviews, 2*, 6032. doi:10.3402/nano.v2i0.6032.
15. Gras, S. L. (2009). Surface- and solution-based assembly of amyloid fibrils for biomedical and nanotechnology applications. *Advances in Chemical Engineering, 35*, 161–209.
16. Gras, S. L., Tickler, A. K., Squires, A. M., Devlin, G. L., Horton, M. A., Dobson, C. M., et al. (2008). Functionalised amyloid fibrils for roles in cell adhesion. *Biomaterials, 29*, 1553–1562.
17. Gazit, E. (2007). Self-assembled peptide nanostructures: The design of molecular building blocks and their technological utilization. *Chemical Society Reviews, 36*, 1263–1269.

18. Zhang, S., Marini, D. M., Hwang, W., & Santoso, S. (2002). Design of nanostructured biological materials through self-assembly of peptides and proteins. *Current Opinion in Chemical Biology, 6*, 865–871.
19. Pernow, B. (1983). Substance P. *Pharmacological Reviews, 35*, 85–141.
20. Severini, C., Improta, G., Falconieri-Erspamer, G., Salvadori, S., & Erspamer, V. (2002). The tachykinin peptide family. *Pharmacological Reviews, 54*, 285–322.
21. Schwyzer, R. (1987). Membrane-assisted molecular mechanism of neurokinin receptor subtype selection. *EMBO Journal, 6*, 2255–2259.
22. Grace, C. R., & Cowsik, S. M. (2011). Solution conformation of non-mammalian tachykinin physalaemin in lipid micelles by NMR. *Biopolymers, 96*, 252–259.
23. Maggio, J. E. (1988). Tachykinins. *Annual Review of Neuroscience, 11*, 13–28.
24. Helke, C. J., Krause, J. E., Mantyh, P. W., Couture, R., & Bannon, M. J. (1990). Diversity in mammalian tachykinin peptidergic neurons: Multiple peptides, receptors, and regulatory mechanisms. *FASEB Journal, 4*, 1606–1615.
25. Merighi, A., Polak, J. M., Gibson, S. J., Gulbenkian, S., Valentino, K. L., & Peirone, S. M. (1988). Ultrastructural studies on calcitonin gene-related peptide-, tachykinins- and somatostatin-immunoreactive neurones in rat dorsal root ganglia: Evidence for the colocalization of different peptides in single secretory granules. *Cell and Tissue Research, 254*, 101–109.
26. Ma, G. Q., Wang, B., Wang, H. B., Wang, Q., & Bao, L. (2008). Short elements with charged amino acids form clusters to sort protachykinin into large dense-core vesicles. *Traffic, 9*, 2165–2179.
27. Yankner, B. A., Duffy, L. K., & Kirschner, D. A. (1990). Neurotrophic and neurotoxic effects of amyloid β protein: Reversal by tachykinin neuropeptides. *Science, 250*, 279–282.
28. El-Agnaf, O. M., Irvine, G. B., Fitzpatrick, G., Glass, W. K., & Guthrie, D. J. (1998). Comparative studies on peptides representing the so-called tachykinin-like region of the Alzheimer Aβ peptide [Aβ(25-35)]. *Biochemical Journal, 336*(Pt 2), 419–427.
29. Kowall, N. W., Beal, M. F., Busciglio, J., Duffy, L. K., & Yankner, B. A. (1991). An in vivo model for the neurodegenerative effects of β amyloid and protection by substance P. *Proceedings of the National Academy of Science of the United States of America, 88*, 7247–7251.
30. Fernandez-Escamilla, A. M., Rousseau, F., Schymkowitz, J., & Serrano, L. (2004). Prediction of sequence-dependent and mutational effects on the aggregation of peptides and proteins. *Nature Biotechnology, 22*, 1302–1306.
31. Maurer-Stroh, S., Debulpaep, M., Kuemmerer, N., de la Paz, M. L., Martins, I. C., Reumers, J., et al. (2010). Exploring the sequence determinants of amyloid structure using position-specific scoring matrices. *Nature Methods, 7*, 237–242.
32. Suk, J. Y., Zhang, F., Balch, W. E., Linhardt, R. J., & Kelly, J. W. (2006). Heparin accelerates gelsolin amyloidogenesis. *Biochemistry, 45*, 2234–2242.
33. Kisilevsky, R. (2000). Review: Amyloidogenesis—Unquestioned answers and unanswered questions. *Journal of Structural Biology, 130*, 99–108.
34. Yamamoto, S., Yamaguchi, I., Hasegawa, K., Tsutsumi, S., Goto, Y., Gejyo, F., et al. (2004). Glycosaminoglycans enhance the trifluoroethanol-induced extension of β2-microglobulin-related amyloid fibrils at a neutral pH. *Journal of the American Society of Nephrology, 15*, 126–133.
35. Cohlberg, J. A., Li, J., Uversky, V. N., & Fink, A. L. (2002). Heparin and other glycosaminoglycans stimulate the formation of amyloid fibrils from α-synuclein in vitro. *Biochemistry, 41*, 1502–1511.
36. Supattapone, S. (2004). Prion protein conversion in vitro. *Journal of Molecular Medicine, 82*, 348–356.
37. Goedert, M., Jakes, R., Spillantini, M. G., Hasegawa, M., Smith, M. J., & Crowther, R. A. (1996). Assembly of microtubule-associated protein tau into Alzheimer-like filaments induced by sulphated glycosaminoglycans. *Nature, 383*, 550–553.
38. Maji, S. K., Schubert, D., Rivier, C., Lee, S., Rivier, J. E., & Riek, R. (2008). Amyloid as a depot for the formulation of long-acting drugs. *PLoS Biology, 6*, e17.
39. Kolset, S. O., Prydz, K., & Pejler, G. (2004). Intracellular proteoglycans. *Biochem Journal, 379*, 217–227.
40. Zanini, A., Giannattasio, G., Nussdorfer, G., Margolis, R. K., Margolis, R. U., & Meldolesi, J. (1980). Molecular organization of prolactin granules. II. Characterization of glycosaminoglycans and glycoproteins of the bovine prolactin matrix. *Journal of Cell Biology, 86*, 260–272.
41. Maji, S. K., Amsden, J. J., Rothschild, K. J., Condron, M. M., & Teplow, D. B. (2005). Conformational dynamics of amyloid β-protein assembly probed using intrinsic fluorescence. *Biochemistry, 44*, 13365–13376.
42. Lakowicz, J. R. (1999). *Principles of fluorescence spectroscopy* (2nd ed.). New York: Kluwer/Plenum.
43. Buck, M. (1998). Trifluoroethanol and colleagues: Cosolvents come of age. Recent studies with peptides and proteins. *Quarterly Reviews of Biophysics, 31*, 297–355.
44. Fezoui, Y., & Teplow, D. B. (2002). Kinetic studies of amyloid β-protein fibril assembly—Differential effects of α-helix stabilization. *Journal of Biological Chemistry, 277*, 36948–36954.
45. Anderson, V. L., Ramlall, T. F., Rospigliosi, C. C., Webb, W. W., & Eliezer, D. (2010). Identification of a helical intermediate in trifluoroethanol-induced alpha-synuclein aggregation. *Proceedings of the National Academy of Sciences of the United States of America, 107*, 18850–18855.
46. Munishkina, L. A., Phelan, C., Uversky, V. N., & Fink, A. L. (2003). Conformational behavior and aggregation of α-synuclein in organic solvents: Modeling the effects of membranes. *Biochemistry, 42*, 2720–2730.
47. Hardy, J., & Selkoe, D. J. (2002). Medicine—The amyloid hypothesis of Alzheimer's disease: Progress and problems on the road to therapeutics. *Science, 297*, 353–356.
48. Klein, W. L., Stine, W. B., Jr, & Teplow, D. B. (2004). Small assemblies of unmodified amyloid β-protein are the proximate neurotoxin in Alzheimer's disease. *Neurobiology of Aging, 25*, 569–580.
49. Winner, B., Jappelli, R., Maji, S. K., Desplats, P. A., Boyer, L., Aigner, S., et al. (2011). In vivo demonstration that α-synuclein oligomers are toxic. *Proceedings of the National Academy of Sciences of the United Sciences of America, 108*, 4194–4199.
50. Kayed, R., Head, E., Thompson, J. L., McIntire, T. M., Milton, S. C., Cotman, C. W., et al. (2003). Common structure of soluble amyloid oligomers implies common mechanism of pathogenesis. *Science, 300*, 486–489.
51. Mosmann, T. (1983). Rapid colorimetric assay for cellular growth and survival: application to proliferation and cytotoxicity assays. *Journal of Immunological Methods, 65*, 55–63.
52. Harper, J. D., & Lansbury, P. T., Jr. (1997). Models of amyloid seeding in Alzheimer's disease and scrapie: Mechanistic truths and physiological consequences of the time-dependent solubility of amyloid proteins. *Annual Review of Biochemistry, 66*, 385–407.
53. Wright, C. F., Teichmann, S. A., Clarke, J., & Dobson, C. M. (2005). The importance of sequence diversity in the aggregation and evolution of proteins. *Nature, 438*, 878–881.
54. Han, H. Y., Weinreb, P. H., & Lansbury, P. T. (1995). The core Alzheimer's peptide Nac forms amyloid fibrils which seed and

are seeded by β-Amyloid—Is NAC a common trigger or target in neurodegenerative disease? *Chemistry & Biology, 2*, 163–169.
55. Cherny, I., & Gazit, E. (2008). Amyloids: Not only pathological agents but also ordered nanomaterials. *Angewandte Chemie (International ed. in English), 47*, 4062–4069.
56. Hamodrakas, S. J. (2011). Protein aggregation and amyloid fibril formation prediction software from primary sequence: Towards controlling the formation of bacterial inclusion bodies. *FEBS Journal, 278*, 2428–2435.
57. Kyte, J., & Doolittle, R. F. (1982). A simple method for displaying the hydropathic character of a protein. *Journal of Molecular Biology, 157*, 105–132.
58. Chou, P. Y., & Fasman, G. D. (1978). Prediction of the secondary structure of proteins from their amino acid sequence. *Advances in Enzymology and Related Areas of Molecular Biology, 47*, 45–148.
59. Monsellier, E., Ramazzotti, M., Taddei, N., & Chiti, F. (2010). A computational approach for identifying the chemical factors involved in the glycosaminoglycans-mediated acceleration of amyloid fibril formation. *PLoS One, 5*, e11363.
60. Valle-Delgado, J. J., Alfonso-Prieto, M., de Groot, N. S., Ventura, S., Samitier, J., Rovira, C., et al. (2010). Modulation of Aβ42 fibrillogenesis by glycosaminoglycan structure. *FASEB Journal, 24*, 4250–4261.
61. Bourgault, S., Solomon, J. P., Reixach, N., & Kelly, J. W. (2011). Sulfated glycosaminoglycans accelerate transthyretin amyloidogenesis by quaternary structural conversion. *Biochemistry, 50*, 1001–1015.
62. Meng, F., Abedini, A., Song, B., & Raleigh, D. P. (2007). Amyloid formation by pro-islet amyloid polypeptide processing intermediates: Examination of the role of protein heparan sulfate interactions and implications for islet amyloid formation in type 2 diabetes. *Biochemistry, 46*, 12091–12099.
63. Sadqi, M., Hernandez, F., Pan, U. M., Perez, M., Schaeberle, M. D., Avila, J., et al. (2002). α-helix structure in Alzheimer's disease aggregates of tau-protein. *Biochemistry, 41*, 7150–7155.
64. Paci, E., Gsponer, J., Salvatella, X., & Vendruscolo, M. (2004). Molecular dynamics studies of the process of amyloid aggregation of peptide fragments of transthyretin. *Journal of Molecular Biology, 340*, 555–569.
65. Abedini, A., & Raleigh, D. P. (2009). A critical assessment of the role of helical intermediates in amyloid formation by natively unfolded proteins and polypeptides. *Protein Engineering, Design and Selection, 22*, 453–459.